Published in final edited form as:
Neuroimage. 2012 March ; 60(1): 279–289. doi:10.1016/j.neuroimage.2011.11.081.

A general analysis of calibrated BOLD methodology for measuring $CMRO_2$ responses: comparison of a new approach with existing methods

Nicholas P. Blockley[1], **Valerie E. M. Griffeth**[2], and **Richard B. Buxton**[1,3]

[1]Center for Functional Magnetic Resonance Imaging, Department of Radiology, University of California San Diego, La Jolla, CA, USA

[2]Department of Bioengineering and Medical Scientist Training Program, University of California San Diego, La Jolla, CA, USA

[3]Kalvi Institute for Brain and Mind, University of California San Diego, La Jolla, CA, USA

Abstract

The amplitude of the BOLD response to a stimulus is not only determined by changes in cerebral blood flow (CBF) and oxygen metabolism ($CMRO_2$), but also by baseline physiological parameters such as haematocrit, oxygen extraction fraction (OEF) and blood volume. The calibrated BOLD approach aims to account for this physiological variation by performing an additional calibration scan. This calibration typically consists of a hypercapnia or hyperoxia respiratory challenge, although we propose that a measurement of the reversible transverse relaxation rate, R_2', might also be used. A detailed model of the BOLD effect was used to simulate each of the calibration experiments, as well as the activation experiment, whilst varying a number of physiological parameters associated with the baseline state and response to activation. The effectiveness of the different calibration methods was considered by testing whether the BOLD response to activation scaled by the calibration parameter combined with the measured CBF provides sufficient information to reliably distinguish different levels of $CMRO_2$ response despite underlying physiological variability. In addition the effect of inaccuracies in the underlying assumptions of each technique were tested, e.g. isometabolism during hypercapnia.

The three primary findings of the study were: 1) The new calibration method based on R_2' worked reasonably well, although not as well as the ideal hypercapnia method; 2) The hyperoxia calibration method was significantly worse because baseline haematocrit and OEF must be assumed, and these physiological parameters have a significant effect on the measurements; and 3) the venous blood volume change with activation is an important confounding variable for all of the methods, with the hypercapnia method being the most robust when this is uncertain.

Keywords

Calibrated BOLD; Cerebral metabolic rate of oxygen; Functional MRI; Hypercapnia; Hyperoxia

Address for correspondence: Nicholas Blockley, University of California San Diego, Radiology - Center for Functional MRI, 9500 Gilman Drive #0677, La Jolla, CA 92093-0677, USA. **Telephone No.:** +1 858 822 0572 **Fax No.:** +1 858 822 0605 nblockley@ucsd.edu.

Introduction

The BOLD signal is dependent on changes in cerebral blood flow (CBF) and oxidative metabolism ($CMRO_2$). However, changes in CBF and $CMRO_2$ alone do not determine the amplitude of the BOLD response to neural activity. It is therefore possible to measure BOLD responses with different amplitudes that result from the same underlying changes in CBF and $CMRO_2$. The scale of the BOLD response is determined by the baseline physiological state of the tissue contained within the imaging voxel. This baseline is characterised by the total amount of deoxyhaemoglobin present, which is dependent on the haematocrit, baseline oxygen extraction fraction (OEF), and baseline blood volume. The calibrated BOLD approach (Davis et al., 1998) was proposed to measure changes in $CMRO_2$ using measurements of CBF and BOLD. This is achieved by characterising differences in baseline physiology using a calibration experiment. Traditionally this experiment consists of simultaneous measurements of CBF and BOLD acquired during interleaved periods of normocapnia and hypercapnia (Davis et al., 1998; Hoge et al., 1999). Hypercapnia is induced by presenting the participant with carbon dioxide rich gas mixture (typically 5% CO_2, 21% O_2, 74% N_2) and results in an increase in CBF and the BOLD signal. A model of the BOLD signal is then used to convert these changes into a measure of the baseline physiological state (Davis et al., 1998), under the assumption that baseline $CMRO_2$ is not altered by hypercapnia (Sicard and Duong, 2005; Jain et al., 2011).

More recently an alternative respiratory challenge was presented whereby hypercapnia was replaced with hyperoxia (Chiarelli et al., 2007). Experiments have been performed with oxygen content ranging from 25% (Mark et al., 2011) to 100% (Chiarelli et al., 2007; Goodwin et al., 2009). Hyperoxia does not substantially increase arterial blood oxygen saturation, but does increase the oxygen carried by arterial blood through an increased plasma oxygen concentration. This results in an increase in venous blood oxygen saturation and hence an increase in BOLD signal. A modification of the BOLD signal model used for hypercapnia calibration can then be used to characterise the baseline state (Chiarelli et al., 2007).

However, respiratory challenges are time consuming to set up, uncomfortable and may be contraindicated for some subjects, for example in Chronic Obstructive Pulmonary Disease (COPD) (Moore et al., 2009). Therefore, it would be useful to be able to calibrate without administering gases. It has long been known that the reversible transverse relaxation rate, R_2', is sensitive to venous cerebral blood volume (CBVv) and the concentration of deoxyhaemoglobin ([*dHb*]) (Yablonskiy and Haacke, 1994). This sensitivity is exploited by the qBOLD approach to make absolute measurements of resting CBVv and OEF (He and Yablonskiy, 2006). However, this method has poor temporal resolution and is not suitable for measuring $CMRO_2$ changes on short timescales. Nevertheless, R_2' is dependent on haematocrit, OEF and blood volume and as such captures most of the characteristics of the baseline physiological state that are important for determining the scaling of the BOLD response, particularly total deoxyhaemoglobin content. Can we therefore use this information to calibrate the BOLD response? In this study we investigate whether R_2' can be used to calibrate the BOLD response through detailed simulation. In addition, we compare this new calibration method with the existing respiratory challenge calibrations, hypercapnia and hyperoxia. The simplifying assumptions of each of these methods are investigated and the uncertainty they introduce into the calibration process assessed.

Theory

A General Model for Calibrated BOLD

The aim of calibrated BOLD is to take measurements of BOLD signal and CBF and combine them with information about the baseline state to estimate $CMRO_2$ changes. This baseline information is gathered from a calibration experiment. In the classic approach introduced by Davis and colleagues, the BOLD response is modeled as:

$$\delta s = M \left[1 - f^{\alpha} \left(\frac{r}{f} \right)^{\beta} \right] \quad (1)$$

where δs is the percentage BOLD signal change, f is the CBF ratio and r is the $CMRO_2$ ratio (activation/baseline), and α and β are model parameters. The calibration parameter M that scales the BOLD signal is calculated from the measured BOLD and CBF responses to hypercapnia, with the assumption of no change in $CMRO_2$ (r=1). Physically, the calibration parameter M depends on a number of physiological variables that affect the local deoxyhemoglobin concentration in the baseline state, and so represents an important source of variation across subjects and across brain regions. It also depends on image acquisition parameters, so that M is not simply a property of the brain, and comparing M values across different studies requires some care.

In the current study our goal is take a more general approach to the process of calibration, as a way of accounting for variations in the baseline state, without assuming the simple form of the Davis model. More generally the calibrated BOLD experiment can be stated in the following way,

$$\delta s = B \; h(f, r) \quad (2)$$

where B is the calibration parameter and $h(f,r)$ is a function that describes the effect of normalised changes in CBF and $CMRO_2$, on the change in BOLD signal. To model h we use a recently described detailed model for the BOLD response that includes a number of physiological variables that were not included in the original Davis model (Griffeth and Buxton, 2011). The model includes three blood compartments (arterial, capillary and venous) as well as the extravascular compartment, and models BOLD signal contributions from all compartments as well as effects of volume exchange as a blood compartment expands. The model also allows the baseline blood volume fractions to be varied, as well as the volume changes of these vascular compartments with activation. Baseline oxygen extraction fraction and blood haematocrit also can be varied. Although this model does not provide a simple closed form for $h(f,r)$ like Eq. (1), it provides a flexible way to simulate the BOLD response for a wide range of physiological baseline states. The model is described in more detail in the Appendix.

The detailed model allows us to test any proposed method for calibration in the following way. The calibration experiment itself is simulated with the detailed BOLD model for a given set of baseline physiological parameters, and the value of B is calculated for the prescribed calibration method from the simulated BOLD and CBF responses. The activation experiment is then simulated for particular values of f and r with the same baseline physiological parameters, and the BOLD response normalized to the calibration parameter ($\delta s/B$) is then plotted as a function of f. This plot represents a simulation of the measured results of a calibrated BOLD study. This procedure is then repeated for many variations of the baseline physiological parameters and the CBF change f, but for the same $CMRO_2$ change r, with each simulation plotted as one point in the $\delta s/B$ vs. f plot. If the calibration is perfect, these points for a constant r should fall on a single curve, and when the simulations

are repeated for a different value of r the points should fall on a distinctly different curve. In this way the calibration completely captures the variability due to the baseline state and the measurements of $\delta s/B$ and f uniquely define r. Note that the shape of the curve for a particular value of r, which effectively is determined by h, is not what we are after here. Instead, the central question is whether a calibration method produces a clean separation of the points for different values of r.

As an initial demonstration of the importance of calibration, Fig. 1 omits calibration and plots δs versus f. Three different levels of $CMRO_2$ change are displayed; 10%, 20% and 30% increases. When baseline haematocrit, Hct, oxygen extraction fraction, E_0, and blood volume, V, are randomly varied across the physiological range, all three $CMRO_2$ levels overlap and cannot be clearly separated. A calibration experiment is therefore required to determine B and to reduce the uncertainty in r. This commonly takes the form of a hypercapnia or hyperoxia respiratory challenge, although here we also consider an alternative technique based on measurements of R_2'.

Hypercapnia Calibration

Hypercapnia calibration is performed by presenting a hypercapnic gas mixture to the participant whilst measurements of BOLD signal and CBF are made (Davis et al., 1998). These measurements are combined with the Davis model to estimate the calibration parameter B with Eq (3). Typically this is known as M, with subscript hc added here to distinguish hypercapnia from hyperoxia.

$$B \equiv M_{hc} = \frac{\delta s}{1 - f^{\alpha-\beta} \quad r^{\beta}} \tag{3}$$

Here, the constants α and β represent flow-volume coupling (Grubb et al., 1974) and the relationship between blood oxygenation and the BOLD signal (Ogawa et al., 1993), respectively. Current practice sets the value of α as 0.2 based on measurements of CBVv, the vascular compartment that underlies the BOLD response (Chen and Pike, 2009). Similarly β is chosen to be 1.3 for experiments performed at 3.0 T (Mark et al., 2011). In the ideal calibration experiment it is assumed that $CMRO_2$ is not altered by hypercapnia (r=1) and this was initially assumed in these simulations.

Hyperoxia Calibration

Hyperoxia calibration is performed in a similar manner to hypercapnia calibration, by presenting a hyperoxic gas mixture to the participant whilst recording measurements of BOLD and CBF (Chiarelli et al., 2007). The BOLD scaling parameter is termed M_{ho} and is equivalent to B in Eq. (2). In the ideal experiment it is assumed that CBF does not change during hyperoxia, in which case measurements of CBF are not necessary during calibration. Hence,

$$B \equiv M_{ho} = \frac{\delta s}{1 - \left(\frac{[dHb]}{[dHb]_0}\right)^{\beta}} \tag{4}$$

where β takes the same definition as for hypercapnia calibration and $[dHb]/[dHb]_0$ is the change in deoxyhaemoglobin concentration due to breathing the hyperoxic gas mixture, relative to normoxia (Chiarelli et al., 2007). To calculate M_{ho} using Eq. (4) $[dHb]/[dHb]_0$ must be estimated. This is achieved using a model of the oxygen carrying capacity of the blood that is a function of the arterial partial pressure of oxygen (PaO_2). In practice this is inferred from the end-tidal pressure of oxygen ($P_{ET}O_2$) expired by the participant, taking into

account alveolar-arterial oxygen gradient and assuming that the arterial blood is well equilibrated with the gas in the alveoli. This latter assumption relies upon healthy lung function for validity. Oxygen is mostly carried bound to haemoglobin within the blood, however a small amount is carried by the plasma. The PaO_2 of the blood determines how much is carried by both of these compartments. The oxygen carried by the plasma is a linear function of PaO_2 ($\varepsilon\ PaO_2$) and for bound oxygen the haemoglobin saturation of arterial blood (SaO_2) can be calculated from an approximation for the oxygen dissociation curve (Severinghaus, 1979):

$$SaO_2 = \frac{1}{\frac{23400}{(PaO_2)^3 + 150 PaO_2} + 1} \tag{5}$$

During hyperoxia the amount of oxygen carried bound to haemoglobin in the arteries increases slightly, alongside a larger increase in the amount carried as dissolved gas in plasma. Therefore, under hyperoxia the amount of oxygen carried by plasma contributes to a greater degree to the overall delivery of oxygen than during normoxia due to the asymptotic nature of Eq. (5). During passage through the capillary bed the extraction of the excess oxygen in plasma offsets the extraction of oxygen bound to haemoglobin, so that venous haemoglobin saturation increases. However, in the venous blood the partial pressure of oxygen (PvO_2) remains low and represents less than 1% of total amount of oxygen carried by venous blood. Therefore, assuming that PvO_2 is negligible should not result in a large error and allows $[dHb]/[dHb]_0$ to be estimated as:

$$\frac{[dHb]}{[dHb]_0} = 1 + \frac{\Delta[dHb]}{[dHb]_0} = 1 + \frac{\phi\ [Hb]\ \Delta SaO_2 - \varepsilon\ \Delta PaO_2}{\phi\ [Hb]\ \{1 - SaO_2\ (1 - E_0)\} - \varepsilon\ PaO_2} \tag{6}$$

where ϕ is the oxygen carrying capacity of haemoglobin (1.34 $mlO_2\ g_{Hb}^{-1}$), ε is the solubility coefficient of oxygen in blood (0.0031 $mlO_2\ dl^{-1}\ mmHg^{-1}$), and ΔSaO_2 and ΔPaO_2 are the change in these parameters due to hyperoxia relative to the normoxic state. Haemoglobin concentration, $[Hb]$, is assumed to be 15 $g_{Hb}\ dl^{-1}$ (Chiarelli et al., 2007; Mark et al., 2011) and the oxygen extraction fraction, E_0, is assumed to be 0.3 (Mark et al., 2011). This value of E_0 is lower than the generally reported values of approximately 0.4 (Perlmutter et al., 1987), however we retain this value to reflect current practice in the papers describing the hyperoxia calibration method. Haemoglobin concentration can be converted to haematocrit using a simple approximation, $Hct \approx 0.03 \times [Hb]$. In summary, the hyperoxia calibration method requires assumed values for several variables. Oxygen carrying capacity and solubility are standard physical parameters that should not vary across subjects. However, haematocrit may well vary across subjects, and baseline O_2 extraction fraction could also vary across brain regions within the same subject.

R_2' Calibration

Analytical results (Yablonskiy and Haacke, 1994) and Monte Carlo (Ogawa et al., 1993) simulations have shown that R_2' is a function of blood volume, haematocrit and OEF.

$$R_2' = \kappa\ V\ (Hct\ E_0)^{\beta} \tag{7}$$

The constant κ subsumes various properties of brain tissue including vessel geometry, magnetic field strength and the susceptibility difference between blood and tissue, and β follows the same definition as in hypercapnia and hyperoxia calibration. If we consider the BOLD signal to be a largely extravascular effect then changes in R_2' determine changes in the BOLD signal. Hence the maximum BOLD signal change during activation is determined by R_2' in the baseline state. Assuming monoexponential decay, the gradient echo (GE) and

spin echo (SE) signal at the BOLD echo time, *TE*, can be described by the following equations, where $R_2^*=R_2+R_2'$.

$$S_{GE}(TE)=S(0)\,e^{-TE\quad\left(R_2+R_2'\right)} \tag{8a}$$

$$S_{SE}(TE)=S(0)\quad e^{-TE\quad R_2} \tag{8b}$$

We propose to use the ratio of these signals to define the calibration parameter *B*.

$$B\equiv\ln\frac{S_{SE}(TE)}{S_{GE}(TE)}=TE\quad R_2' \tag{9}$$

The echo time, *TE*, is included to account for the echo time dependence of the magnitude of the BOLD response. This approach assumes that intravascular signal contributions are negligible and that diffusional narrowing does not dominate. These assumptions were tested using an extension of the detailed BOLD signal model (Griffeth and Buxton, 2011). This was achieved by considering the signal contributions from each of the compartments of the detailed signal model under GE and SE pulse sequences during a resting baseline and is described in detail in the Appendix. It must be noted that the measured value of R_2' is dependent on the way in which it is measured. It is generally assumed that the transverse signal decay of a homogenous voxel is monoexponential. However, for time points close to the excitation pulse in a GE sequence, and close to the refocusing pulse for a SE sequence, this decay has been shown to be quadratically exponential in nature (Yablonskiy and Haacke, 1994). In the case of Eq. (9) the SE signal will be acquired in this short echo time regime while the GE signal will be acquired in the long echo time regime. Models for the SE signal compartments were chosen to be consistent with the short echo time regime (Zhao et al., 2007; Uludağ et al., 2009).

Methods

Simulations

The detailed signal model was used to simulate calibration using hypercapnia, hyperoxia and R_2' using Eqs (3), (4) and (9), respectively, as prescriptions for taking specific measured signals and calculating *B*. Note that the first two methods explicitly depend on the parameter β, which functions as a way to approximate multiple factors affecting the BOLD response. This parameter does not appear in the detailed BOLD model because these different mechanisms are individually modeled. Similarly, the parameter α is related to CBVv change, and in the detailed model the changes in different vascular compartments are simulated.

All simulations were performed in MATLAB (Mathworks, Natick, MA). The main aim of these simulations was to determine how variability in physiology affects the uncertainty in a measurement of $CMRO_2$. For variations in a single parameter simulations are performed by propagating linearly spaced values of this parameter through the detailed signal model. However, for variations in baseline physiology we expect multiple parameters to vary simultaneously and the compound effect of these variations isn't clear. Simple linear ranges for multiple parameters would be slow and produce multidimensional data that is difficult to visualise. Here we take an alternative approach by drawing random combinations of these parameters from predefined ranges. Multiple repeats of this process enable a ‘cloud’ of data to be generated that can be visualised in two dimensions, as shown in Fig. 1.

In order to investigate the sensitivity of each of the calibration methods to baseline physiological variability and the assumptions of each method, the change in BOLD signal was divided by the calibration scaling factor. In the following figures this quantity, $\delta s/B$, is plotted against f. These simulations are performed for two different scenarios; fixed $CMRO_2$ level or fixed CBF-$CMRO_2$ coupling value, n, defined as,

$$n=\frac{f-1}{r-1}. \tag{10}$$

Fixed $CMRO_2$ changes enables us to visualise how well different $CMRO_2$ levels can be separated, whilst fixed CBF-$CMRO_2$ coupling shows the uncertainty in these measurements for more physiologically plausible combinations of CBF and $CMRO_2$. Fixed $CMRO_2$ levels of 10%, 20% and 30% increases and CBF-$CMRO_2$ coupling values of n = 1.3, 2 and 3 were simulated. An n value of 1.3 represents a special case where the increase in blood oxygenation due to increased CBF is approximately balanced by increased oxygen extraction due to metabolism, resulting in a net zero BOLD signal change. The exact value of n required to achieve this condition is CBF dependent and can be estimated from the Davis model (Eq. (1)) for specific values of α and β. Therefore, n=1.3 is an approximate BOLD-nulling value for the CBF values simulated.

Each of the calibration parameter values was calculated as described in the Theory section. In summary, the hypercapnia calibration scaling factor, M_{hc}, is calculated using Eq. (3) under the assumption that $CMRO_2$ does not change (r=1) and a 47% increase in CBF due to hypercapnia (f=1.47). In all simulations α in Eq. (3) was chosen to be 0.2. The hyperoxia calibration, M_{ho}, is calculated using Eq. (4), relying on Eq. (6) to determine $[dHb]/[dHb]_0$, following the method of Mark *et al*., and $[Hb]$ and E_0 in this equation have fixed values of 15 g_{Hb} dl^{-1} and 0.3, respectively (Mark et al., 2011). Hyperoxia calibration was simulated as an ideal experiment where CBF is not altered by hyperoxia. In both traditional methods β was chosen to be 1.3. In R_2' calibration the scaling factor is the product of TE and R_2', and is calculated using Eq. (9). No assumptions about isometabolism or the value of α and β are required.

Baseline Physiological Variation

The parameters that determine the baseline state are haematocrit, baseline OEF and baseline blood volume. Haematocrit is known to vary between males and females with typical ranges of 0.42 – 0.50 and 0.37 – 0.47, respectively (McPhee and Hammer, 2009). However, there is a great deal of overlap and typically calibration methods do not take account of sex during data processing, therefore a range of 0.37 – 0.50 was tested. Ranges for baseline OEF are similarly wide at 0.35 – 0.55 (Marchal et al., 1992). This range was extended at the low end to encompass the assumed OEF value of 0.3 used in the hyperoxia calibration method. The baseline total blood volume fraction is typically measured to be 0.05 in grey matter (Roland et al., 1987). However, to account for the partial volume effect at the low end of the range and for incorporation of large vessels at the high end of the range a total blood volume fraction between 0.01 and 0.1 was tested. Relative volume fractions for arteries, capillaries and veins were fixed at 0.2, 0.4 and 0.4, respectively. This resulted in simulated venous volume fractions in the range 0.004 to 0.04. Finally, the activation induced change in CBF was simulated across a large range (0.8 to 1.8) to encompass all physiologically plausible eventualities. Values for the remaining model parameters are listed in Table 1.

Randomly generated combinations of these parameters were selected from their respective ranges, including activation induced CBF change, using a uniform random number generator. A uniform random distribution was chosen as the mean and standard deviation of each of the physiological parameters is not generally known. For each simulation 1,000

repeats of the random parameter generation process were completed. These values were propagated through the detailed signal model to generate a stimulus induced BOLD signal change, δs, and a calibration parameter, B, for each calibration method. To simplify the simulation process CBF was included as an additional randomly generated value providing the third experimental variable of the calibrated BOLD approach.

Flow-Volume Coupling Assumption

A general assumption of all calibrated BOLD methods is that changes in CBVv can be inferred from measurements of CBF through a power law relationship defined by α. An inaccurate value of α would be a source of systematic error. Here we aim to determine the sensitivity of each of the calibration methods to the value of α. Traditionally α was defined as 0.4 based on measurements of total CBV (Grubb et al., 1974), but has more recently been superseded by a value of 0.2 using measurements of venous CBV change (Chen and Pike, 2009). These values were used to test the extremes of the range for flow-volume coupling given our current knowledge. When calculating M_{hc}, α in Eq. (3) was fixed at 0.2 regardless of the value of the underlying flow-volume coupling. This reflects the way that hypercapnia calibration is performed, whereby a value of α must be assumed that may not reflect the true underlying changes in volume.

Effect of Errors in Assumptions

Assumptions that would lead to the largest sources of error in each method were identified and the effect of systematic error in these assumptions was tested. Baseline physiological variability was not included in these simulations, unless otherwise stated, and standard values for these parameters were assumed (Hct=0.45, E_0=0.4, $V_{I,0}$=0.05).

It has been shown by a number of experiments that hypercapnia may cause a reduction in baseline $CMRO_2$ (Xu et al., 2010). It is normally assumed that there is no change in $CMRO_2$ due to hypercapnia, (r=1). In order to consider the effect of reduced $CMRO_2$ the value of r=0.85 was also simulated to reflect a 15% reduction in $CMRO_2$ during the hypercapnia challenge.

For hyperoxia the estimation of M_{ho} is dependent on the calculation of $[dHb]/[dHb]_0$ from the change in $P_{ET}O_2$ measured during hyperoxia. To simplify this calculation values for $[Hb]$ and E_0 are assumed (Mark et al., 2011). Simulations were performed to determine whether more accurate values of one or both parameters would enable variations in baseline physiology to be better accounted for. Since the accuracy of these assumptions is dependent on physiological variability, the same approach of generating random combinations of baseline parameters as used for baseline physiological variation alone was used.

Measurements of R_2' are not only sensitive to mesoscopic sources of magnetic field inhomogeneity around blood vessels but also to large scale magnetic field inhomogeneity that are not removed during shimming. The sensitivity of R_2' calibration to large scale magnetic field inhomogeneity was tested by simulating (Eq. (A8)) a frequency difference across the voxel, $\Delta\omega$, of 20 Hz (An and Lin, 2003).

Results

Baseline Physiological Variability

Figure 2 displays the effect of normalising the BOLD signal change using a calibration measurement. All three calibration methods drastically reduce the variability in the relationship between BOLD and CBF (cf. Fig. 1). The width of the lines for each $CMRO_2$ level (Fig. 2a-c), or CBF-$CMRO_2$ coupling value (Fig. 2d-e), are proportional to the error in

the final measurement of $CMRO_2$. In an ideal calibration experiment there would be no deviation from the mean and the width of the line would be zero.

For hypercapnia calibration the line width appears to be constant with increasing CBF and independent of the $CMRO_2$ level (Fig. 2a) or CBF-$CMRO_2$ coupling value (Fig. 2d). Hyperoxia calibration shows an increase in the line width with increasing CBF (Fig. 2b,e). The line width is minimised when CBF and $CMRO_2$ balance to give a zero BOLD signal change equivalent to n=1.3 in the plot of CBF-$CMRO_2$ coupling (Fig. 2e). R_2' calibration shows a similar trend to hyperoxia calibration, but with a reduced line width (Fig. 2c,f).

Flow-Volume Coupling Assumption

The effect of assuming that the coupling between CBF and CBVv is accurately known is displayed in Fig. 3. Solid lines are used to represent the case where α=0.2 and dashed lines for when α=0.4. Here we are examining the effect of assuming an incorrect value for α. Therefore, a calibration method with low sensitivity to this parameter should show only a minor shift between these lines, ultimately minimising the error in the measurement of $CMRO_2$.

Hypercapnia shows the smallest shift, representing the lowest sensitivity to an inaccurately assumed value of α (Fig. 3a,d). The magnitude of this shift appears to increase with increasing change in the $CMRO_2$ level (Fig. 3a). Hyperoxia and R_2' calibration both show a larger shift than hypercapnia calibration (Fig. 3b,e; Fig. 3c,f). In all cases the effect of assuming an inaccurate value of α causes the greatest effect for n=1.3 in plots of CBF-$CMRO_2$ coupling.

Hypercapnia Calibration Assumption

Figure 4 considers the effect of a change in baseline $CMRO_2$ during hypercapnia. Solid lines represent r=1 during hypercapnia and dashed lines r=0.85. The shift between these lines appears to increase with $CMRO_2$ level (Fig. 4a) and CBF-$CMRO_2$ coupling (Fig. 4b). Unlike flow-volume coupling, changes in $CMRO_2$ during hypercapnia have little to no effect when n=1.3.

Hyperoxia Calibration Assumptions

Investigation of the origin of the increased variability in hyperoxia calibration is displayed in Fig. 5. Including more accurate information about either haematocrit (Fig. 5a,d) or baseline oxygenation (Fig. 5b,e) reduces this variability. Information about both of these parameters (Fig. 5c,f) reduces variability to similar levels as hypercapnia calibration (Fig. 2a,d).

R_2' Calibration Assumption

Figure 6 considers the effect of large scale magnetic field inhomogeneity on R_2' calibration. Solid lines represent a perfectly homogenous field ($\Delta\omega$=0) and dashed lines represent $\Delta\omega$=20 Hz. The shift between these lines is of a similar order to that seen for $CMRO_2$ change during hypercapnia (Fig. 4).

Discussion

Use of the calibrated BOLD approach has improved the interpretation of fMRI by accounting for physiological variability. Without this calibration procedure measurements of BOLD signal and CBF cannot be used to determine the change in $CMRO_2$ (Fig. 1). However, the extent to which this physiological variability can be characterised by existing methods is not easily accessible in an experimental setting. The simulations performed in this study enable us to investigate these methods and the assumptions that underpin them.

Key to this approach was the use of a detailed model of the BOLD effect that allowed us to vary a number of physiological parameters associated with the baseline state and the response to activation. This allowed us to model effects that were not included in the simpler Davis model standardly used for calibrated BOLD experiments. The effectiveness of the different calibration methods was tested by simulating the calibration experiment as well as the activation experiment, and testing whether the measured BOLD response to activation scaled by the calibration parameter combined with the measured CBF response provides sufficient information to reliably distinguish different levels of $CMRO_2$ response despite underlying physiological variability. We evaluated the original hypercapnia method (Davis et al., 1998), the more recently proposed hyperoxia method (Chiarelli et al., 2007) and a novel method based on R_2'. The simulation methodology used here has previously been used to optimise hypercapnia calibrated BOLD (Griffeth and Buxton, 2011), the results of which have been applied experimentally (Griffeth et al., 2011). Extensions to the detailed signal model allowed us to simulate R_2' in the baseline state, in order to assess its use as an alternative calibration method.

There were three primary findings of this study: 1) The new calibration method based on R_2' worked reasonably well, although not as well as the ideal hypercapnia method; 2) The hyperoxia calibration method was significantly worse because baseline haematocrit and OEF must be assumed, and variability of these physiological parameters has a significant effect on the measurements; and 3) the venous blood volume change with activation is an important confounding variable for all of the methods, with the hypercapnia method being the most robust when this is uncertain. The results for each of the calibration methods tested are discussed in more detail below.

Hypercapnia Calibration

Simulation of hypercapnia calibration revealed that this method provides an accurate calibration for baseline physiological variability (Fig. 2a,d). The broadening of the line due to physiological variability shows only very weak dependence on the change in CBF. Uncertainty in the value of α causes additional deviation of the lines of $CMRO_2$ that appears to increase with increasing $CMRO_2$ change (Fig. 3a,d). We also tested the resulting errors if the assumption of no $CMRO_2$ change with hypercapnia is wrong. When a reduction in $CMRO_2$ during hypercapnia a shift in the lines of $CMRO_2$ was observed (Fig. 4). This could result in an inaccurate measurement of $CMRO_2$, for example when f=1.6 a 10% $CMRO_2$ change when r=0.85 would appear similar to a 20% change when r=1.

Hyperoxia Calibration

Simulations of hyperoxia calibration, when values for baseline [*Hb*] and E_0 are assumed, predict poor performance of this method for normalising the BOLD signal change (Fig. 2b,e). Further investigation revealed that when more information is known, such as [*Hb*] (Fig. 5a,d) or E_0 (Fig. 5b,e), then uncertainty is reduced. When both variables are known then uncertainty is reduced to the same level as hypercapnia calibration (Fig. 5c,f). This uncertainty is minimised when the combination of CBF and $CMRO_2$ changes result in a net zero BOLD signal (as is also the case for R_2' calibration). This effectively means that the venous oxygen saturation is unchanged between the rest and activated states and hence the physiological variability does not have any effect.

The origin of the observed poor performance of hyperoxia calibrated BOLD can be determined by considering Eq. (6). The change in deoxyhaemoglobin concentration due to hyperoxia ($[dHb]/[dHb]_0$) is determined by the decrease in concentration $\Delta[dHb]$ and the baseline concentration $[dHb]_0$. The former is determined by [*Hb*], as this adjusts the balance of oxygen carried by haemoglobin and plasma, and is independent of E_0, whereas the latter

is determined by E_0 at normoxia and is independent of [*Hb*]. Accurate values of [*Hb*] and E_0 are therefore required as $[dHb]/[dHb]_0$ is used to convert measurements of the BOLD signal change during hyperoxia to M_{ho} (Eq. (4)). This conversion is provided by the denominator of Eq. (4) producing a scaling of the BOLD signal change equivalent to one over the denominator. For the extremes of the [*Hb*] and E_0 ranges tested here, and a fixed ΔPaO_2 of 310 mmHg, this scaling value is in the range 5.9 to 15.6 (assuming β=1.3). In contrast, the approach taken by Mark *et al*. (Mark et al., 2011) will always scale the hyperoxic BOLD signal change by 7.9 for the same fixed ΔPaO_2. Whilst the extremes of the [*Hb*] and E_0 ranges are unlikely to simultaneously exist this analysis illustrates the sensitivity of hyperoxia calibration to assumed values for these parameters, and explains the reduced variability encountered when both are known (Fig. 5c,f). Therefore, hyperoxia calibration may be improved by acquiring more accurate information about baseline physiology. This could be achieved by making direct MR measurements of deoxyhaemoglobin concentration in the sagittal sinus as an approximation for E_0 (Jain et al., 2011; Lu et al., 2011) or by measuring the haematocrit from a venous blood sample.

It is unclear whether this expected variability has been observed in the literature, largely due to the limited number of studies having undertaken this calibration. A large spread in the calibration parameter M_{ho} has been observed (Goodwin et al., 2009), which would result from the variability we see, but it is unclear whether the uncontrolled manual hyperoxia challenge employed in this study may have contributed to this effect. Studies using controlled hyperoxic challenges have suggested that the variability in measurements of $CMRO_2$ is lower for hyperoxia calibration when compared with hypercapnia calibration (Mark et al., 2011). The results of our simulations conflict with this observation.

Hyperoxia calibration also shows greater sensitivity to flow-volume coupling than hypercapnia calibration (Fig. 3b,e). The resulting shift in the lines of $CMRO_2$ could result in a large error in the magnitude of the $CMRO_2$ change if the assumed flow-volume coupling does not match the physiological relationship.

R_2' Calibration

The concept of using R_2' to calibrate the BOLD response is based on this parameter's well known dependence on haematocrit, OEF and blood volume (Yablonskiy and Haacke, 1994). Currently this effect is exploited by the qBOLD method to measure baseline blood oxygenation and volume (He and Yablonskiy, 2006). However, to date it has not been used within a calibrated BOLD framework to measure changes in $CMRO_2$ during activation. At first glance it appears that R_2' would be a poor choice for calibration because the BOLD response depends in part on signal changes that would not be captured by R_2'. In a gradient-echo based BOLD experiment the signal change is due largely to changes in the transverse relaxation rate R_2*, which is taken to be a sum of processes that cannot be reversed by a spin-echo (R_2) and processes that can be reversed (R_2'). Motional narrowing due to diffusion of spins around sources of magnetic field heterogeneity means that a good part of the intravascular signal changes and part of the extravascular signal change around the smallest vessels cannot be fully refocused by a spin-echo, and so should not contribute to R_2'. In addition, volume exchange effects as blood vessels expand also contribute to the BOLD effect, but are not directly related to R_2'. Nevertheless, our simulations indicate that R_2' in the baseline state captures much of the physiological variability of the baseline state that does affect the BOLD response. The reason it works as well as it does is probably that R_2' essentially reflects the amount of deoxyhemoglobin in the baseline state, and the other factors affecting the BOLD response for the most part tend to scale with total deoxyhemoglobin.

The main weakness of this calibration method is its sensitivity to magnetic field inhomogeneity. Investigation of a 20 Hz frequency difference across a voxel in one dimension showed that this causes a shift in the lines of $CMRO_2$ that increases with changes in CBF (Fig. 6). The magnitude of this shift is very similar to that caused by $CMRO_2$ changes during hypercapnia calibration. For example, a 10% $CMRO_2$ change when $\Delta\omega$=20 Hz leads to the same R_2' as a 20% change when $\Delta\omega$=0 (f=1.6).

This magnitude of magnetic field inhomogeneity is likely for regions of the brain that are not close to air-tissue interfaces. For regions of the brain closer to the surface, where $\Delta\omega$ is larger, measurements of R_2' will need to be corrected for residual field gradients (Yablonskiy, 1998) or their effect minimised by the acquisition technique (Christen et al., 2010). Experiments using the qBOLD technique have shown that this effect can be corrected enabling R_2' calibrated BOLD to become a practical alternative to hypercapna or hyperoxia (He and Yablonskiy, 2006). The major benefit of this alternative method is a reduction in the complexity of the experimental protocol. Equipment to perform a respiratory challenge is not required, saving time and permitting the calibration scan to be based purely on endogenous contrast.

For this approach to yield an accurate calibration factor it is assumed that deoxyhaemoglobin is the dominant source of paramagnetism in the brain. Other possible sources of iron in the brain include ferritin, transferrin, neuromelanin and haemosiderin (Stankiewicz et al., 2007). However, the sensitivity of R_2' to these sources is also dependent on the geometry of the iron deposition. This effect is maximised in the static dephasing regime where the diffusion length of protons around the susceptibility inclusion is much shorter than the dimension of the inclusion itself. This dimension is approximately equivalent to a cylinder with a radius of 7 μm, but this R_2' contrast falls away rapidly with radius. (Boxerman et al., 1995). Very small scale inclusions, such as ferritin and transferrin, do not produce R_2' contrast and appear as a pure R_2 effect. There are two main conditions in which elevated values of R_2' are measured in the brain; Parkinson's disease and brain haemorrhage. In Parkinson's disease deposits of iron in the substantia nigra, consisting of neuromelanin granules and iron filled Lewy bodies (Castellani et al., 2000), have been shown to result in elevated R_2' measurements (Ordidge et al., 1994). Lewy bodies have a diameter of approximately 8 μm and are likely to exhibit an R_2' effect. Brain haemorrhage causes bleeding into the tissues of the brain and production of haemosiderin, and has also been shown to increase R_2' (Wismer et al., 1988). If R_2' calibration is to be performed in patients with either of these conditions then care must be taken to avoid affected areas of the brain.

Estimating $CMRO_2$ changes

A measurement of $CMRO_2$ change is the ultimate aim of calibrated BOLD, converting information contained in δs, B and f into a measure of r. In the traditional approach the Davis model plays a dual role, first as a way to convert measured hypercapnia responses into a calibration factor, and second as a way to use that factor in combination with measured responses to activation to estimate the $CMRO_2$ change. In the current analysis we have essentially broken the link between the two steps. With this approach we can consider any potential method for calibrating the BOLD signal, and determine an appropriate form of $h(f,r)$ in Eq. (2) through simulations of both the calibration experiment and the activation experiment with the detailed BOLD model. That is, $h(f,r)$ is given implicitly through the detailed model by the curves in the $\delta s/B$ versus f plane (e.g., Fig. 2a and 2c for the hypercapnia and R_2' methods, respectively). An appropriate lookup table, or parameterization of the curves in the Figures, would allow calculation of r for a given set of measurements, effectively defining $h(f,r)$. That is, although the Davis model was used to define the calibration experiment for hypercapnia, this was simply used as a particular recipe

for calculating a value of *B*, and the detailed model was used to simulate that recipe and provide curves of how the measured signals vary with different $CMRO_2$ changes. In this way the detailed model provides a form for $h(f,r)$ that is appropriate for the defined method of calculating *B*. If that method changed (e.g., if the hypercapnia responses were used to calculate *M* with different values of α and β), then the detailed simulations would provide a shifted set of curves defining a new form of $h(f,r)$ appropriate for the new definition of the method for calculating *B*.

Conclusion

The simulations performed in this study enable the potential strengths and weaknesses of BOLD calibration methods to be investigated. In addition, a new calibration method is proposed that does not require a respiratory challenge. Hypercapnia calibration is shown to be robust even when isometabolism during hypercapnia is not assumed and the flow-volume coupling is altered. Simulations of hyperoxia calibration reveal hitherto unexplored weaknesses due to the assumptions that must be made in the model of oxygen transport used to estimate the change in venous blood oxygenation due to hyperoxia. This suggests further experimental validation of this method is required before it may be used routinely. Examination of R_2' as a new calibration method show that such a technique is promising. Whilst the uncertainty in the measurement of $CMRO_2$ may be increased when compared with hypercapnia, this method is more generally applicable to the population at large as it does not require gases to be administered. However, further work is needed to develop robust acquisition methods that allow correction for large scale field inhomogeneity effects.

Additionally, in the absence of measurements of CBF, a measurement of R_2' may also be useful as a normalisation procedure to reduce intersubject variability in the BOLD response. These approaches compare the stimulus evoked BOLD response with measurements of the BOLD response to a hypercapnia challenge (Biswal et al., 2007), or with a single aspect of baseline physiology such as CBF (Liau and Liu, 2009) or baseline blood oxygenation (Lu et al., 2008). A measurement of R_2', however, is sensitive to multiple sources of physiological variability through its sensitivity to blood volume, blood oxygenation and haematocrit and may account for a greater degree of intersubject variability than traditional methods.

Acknowledgments

We would like to thank Aaron Simon, Farshad Moradi and David Dubowitz for helpful discussions regarding this work. This work was supported by funding from NIH/NINDS grant NS-036722.

Appendix

Simulations of the effect of changes in CBF, $CMRO_2$ and baseline physiology were performed using a previously reported detailed BOLD signal model (Griffeth and Buxton, 2011). Constants required for this model are detailed in Table 1. This model was further extended to enable R_2' in the baseline resting state to be simulated. Taking Eq. (8) as a starting point, we can expand these relations to include multiple signal compartments for both gradient echo (GE) and spin echo (SE) pulse sequences.

$$S_{GE}(TE) = \left\{\left(1 - V_{I,0}\right) \; S_{E,0}(0) \; e^{-TE \; \left(R_{2,0}+R^*_{2E}\right)} + V_{A,0} \; S_{A,0}(0) \; e^{-TE \; R^*_{2A}} + V_{C,0} \; S_{C,0}(0) \; e^{-TE \; R^*_{2C}} + V_{V,0} \; S_{V,0}(0) \; e^{-TE \; R^*_{2V}} \; F(TE)\right. \tag{A1a}$$

$$S_{SE}(TE) = \left(1 - V_{I,0}\right) \; S_{E,0}(0) \; e^{-TE \; \left(R_{2,0}+R_{2E}\right)} + V_{A,0} \; S_{A,0}(0) \; e^{-TE \; R_{2A}} + V_{C,0} \; S_{C,0}(0) \; e^{-TE \; R_{2C}} + V_{V,0} \; S_{V,0}(0) \; e^{-TE \; R_{2V}} \quad \text{(A1b)}$$

Here V, $S(0)$, R_2* and R_2 are the volume fraction, proton density and transverse relaxation rates for their respective compartments indicated by subscripts; intravascular (I), extravascular (E), arterial (A), capillary (C) and venous (V). Parameters with subscript 0 reflect the baseline resting value. Monoexponential decay of each compartment is assumed with echo time TE. The extravascular transverse relaxation rate for both GE and SE signals is modelled as a baseline rate ($R_{2,0}$) plus an additive term (R^*_{2E} or R_{2E}). This term reflects dephasing of the signal due to mesoscopic magnetic field inhomogeneity for GE and incomplete refocussing of this dephasing due to diffusional narrowing in the case of the SE. To complete the model, expressions for intra- and extravascular R_2 and R_2* are required along with the definition of $F(TE)$, the signal attenuation due to magnetic field inhomogeneity. Intravascular signal was modelled using measurements of the dependency of R_2* on haematocrit and blood oxygenation saturation (Y) (Zhao et al., 2007).

$$R^*_{2I} = A^* + C^* \quad (1 - Y)^2 \quad \text{(A2)}$$

In order to further generalise the detailed signal model, the dependency of A* and C* on haematocrit (Hct) was approximated by linearly fitting to data acquired at 3.0 T (Zhao et al., 2007; Griffeth and Buxton, 2011).

$$A^* = 14.9 \quad Hct + 14.7 \quad \text{(A3a)}$$

$$C^* = 302.1 \quad Hct + 41.8 \quad \text{(A3b)}$$

Similarly R_2 was modelled based on measurements of the dependency of blood R_2 on oxygenation and haematocrit (Zhao et al., 2007).

$$R_{2I} = A + C \quad (1 - Y)^2 \quad \text{(A4)}$$

$$A = 16.4 \quad Hct + 4.5 \quad \text{(A5a)}$$

$$C = 165.2 \quad Hct + 55.7 \quad \text{(A5b)}$$

These measurements were acquired using a single spin echo pulse sequence, stepped through a range of echo time values, and hence are consistent with the short time regime of transverse signal decay (Yablonskiy and Haacke, 1994). Extravascular R_2* was modelled using the results of Monte Carlo simulations (Ogawa et al., 1993),

$$\Delta R^*_{2E} = a^*_L \quad \Delta\chi \quad Hct \quad \omega_0 \left[V \left| Y_{off} - Y \right| - V_0 \left| Y_{off} - Y_0 \right| \right] \quad \text{for large vessels} \quad \text{(A6a)}$$

$$\Delta R^*_{2E} = a^*_S \quad \Delta\chi \quad Hct \quad \omega_0 \left[V \left| Y_{off} - Y \right|^2 - V_0 \left| Y_{off} - Y_0 \right|^2 \right] \quad \text{for small vessels} \quad \text{(A6b)}$$

where the constants a_L^* and a_S^* scale R_{2E}^* for large and small vessels, respectively, and ω_0 is the proton Larmor frequency. Vessels are categorised as being large with diameters in the range 16 – 200 μm (arterioles and venules) or small (capillaries) with a diameter of 5 μm (Ogawa et al., 1993). Fully oxygenated blood and tissue do not have the same susceptibility and this is reflected by the blood oxygen saturation offset Y_{off}, i.e. the point at which fully oxygenated blood and tissue have the same susceptibility (Spees et al., 2001). The results of Monte Carlo simulations for a single spin echo pulse sequence were used to simulate the extravascular R_2 (Uludağ et al., 2009). These simulations are consistent with the blood R_2 measurements of Zhao *et al*. and with acquisition in the short echo time regime (Yablonskiy and Haacke, 1994). The large vessel relation was derived from simulations of 16 μm diameter vessels (arterioles and venules) and the small vessel relation from vessels (capillaries) of 5 μm diameter.

$$R_{2E} = V_0 \sum_n a_{L,n} \left[\Delta\chi \quad Hct \quad \omega_0 \left| Y_{off} - Y_0 \right| \right]^n \qquad \text{for large vessels} \tag{A7a}$$

$$R_{2E} = V_0 \sum_n a_{S,n} \left[\Delta\chi \quad Hct \quad \omega_0 \left| Y_{off} - Y_0 \right| \right]^n \qquad \text{for small vessels} \tag{A7b}$$

Finally, the signal attenuation of the gradient echo data due to large scale magnetic field inhomogeneity can also be modeled (Yablonskiy, 1998),

$$F(TE) = \frac{\sin(\Delta\omega \quad TE/2)}{(\Delta\omega \quad TE/2)} \tag{A8}$$

where Δω is the frequency difference across the voxel. The constants detailed in these equations are listed in Table 1.

References

An H, Lin W. Impact of intravascular signal on quantitative measures of cerebral oxygen extraction and blood volume under normo- and hypercapnic conditions using an asymmetric spin echo approach. Magn. Reson. Med. 2003; 50:708–716. [PubMed: 14523956]

Biswal BB, Kannurpatti SS, Rypma B. Hemodynamic scaling of fMRI-BOLD signal: validation of low-frequency spectral amplitude as a scalability factor. Magn Reson Imaging. 2007; 25:1358–1369. [PubMed: 17482411]

Boxerman JL, Hamberg LM, Rosen BR, Weisskoff RM. MR contrast due to intravascular magnetic susceptibility perturbations. Magn. Reson. Med. 1995; 34:555–566. [PubMed: 8524024]

Castellani RJ, Siedlak SL, Perry G, Smith MA. Sequestration of iron by Lewy bodies in Parkinson's disease. Acta Neuropathol. 2000; 100:111–114. [PubMed: 10963356]

Chen JJ, Pike GB. BOLD-specific cerebral blood volume and blood flow changes during neuronal activation in humans. NMR Biomed. 2009; 22:1054–1062. [PubMed: 19598180]

Chiarelli PA, Bulte DP, Wise R, Gallichan D, Jezzard P. A calibration method for quantitative BOLD fMRI based on hyperoxia. Neuroimage. 2007; 37:808–820. [PubMed: 17632016]

Christen T, Lemasson B, Pannetier N, Farion R, Segebarth C, Rémy C, Barbier EL. Evaluation of a quantitative blood oxygenation level-dependent (qBOLD) approach to map local blood oxygen saturation. NMR Biomed. 2010; 24:393–403.

Davis TL, Kwong KK, Weisskoff RM, Rosen BR. Calibrated functional MRI: mapping the dynamics of oxidative metabolism. Proc. Natl. Acad. Sci. U.S.A. 1998; 95:1834–1839. [PubMed: 9465103]

Goodwin JA, Vidyasagar R, Balanos GM, Bulte D, Parkes LM. Quantitative fMRI using hyperoxia calibration: Reproducibility during a cognitive Stroop task. Neuroimage. 2009; 47:573–580. [PubMed: 19398018]

Griffeth VEM, Perthen JE, Buxton RB. Prospects for quantitative fMRI: investigating the effects of caffeine on baseline oxygen metabolism and the response to a visual stimulus in humans. Neuroimage. 2011; 57:809–816. [PubMed: 21586328]

Griffeth VEM, Buxton RB. A theoretical framework for estimating cerebral oxygen metabolism changes using the calibrated-BOLD method: Modeling the effects of blood volume distribution, hematocrit, oxygen extraction fraction, and tissue signal properties on the BOLD signal. Neuroimage. 2011; 58:198–212. [PubMed: 21669292]

Grubb RL, Raichle ME, Eichling JO, Ter-Pogossian MM. The effects of changes in PaCO2 on cerebral blood volume, blood flow, and vascular mean transit time. Stroke. 1974; 5:630–639. [PubMed: 4472361]

He X, Yablonskiy DA. Quantitative BOLD: Mapping of human cerebral deoxygenated blood volume and oxygen extraction fraction: Default state. Magn. Reson. Med. 2006; 57:115–126. [PubMed: 17191227]

Hoge RD, Atkinson J, Gill B, Crelier GR, Marrett S, Pike GB. Investigation of BOLD signal dependence on cerebral blood flow and oxygen consumption: the deoxyhemoglobin dilution model. Magn. Reson. Med. 1999; 42:849–863. [PubMed: 10542343]

Jain V, Langham MC, Floyd TF, Jain G, Magland JF, Wehrli FW. Rapid magnetic resonance measurement of global cerebral metabolic rate of oxygen consumption in humans during rest and hypercapnia. J. Cereb. Blood Flow Metab. 2011; 31:1504–1512. [PubMed: 21505481]

Liau J, Liu TT. Inter-subject variability in hypercapnic normalization of the BOLD fMRI response. Neuroimage. 2009; 45:420–430. [PubMed: 19111622]

Lu H, Zhao C, Ge Y, Lewis-Amezcua K. Baseline blood oxygenation modulates response amplitude: Physiologic basis for intersubject variations in functional MRI signals. Magn. Reson. Med. 2008; 60:364–372. [PubMed: 18666103]

Lu H, Xu F, Grgac K, Liu P, Qin Q, van Zijl P. Calibration and validation of TRUST MRI for the estimation of cerebral blood oxygenation. Magn. Reson. Med. 2011 In Press.

Marchal G, Rioux P, Petit-Taboué MC, Sette G, Travère JM, Le Poec C, Courtheoux P, Derlon JM, Baron JC. Regional cerebral oxygen consumption, blood flow, and blood volume in healthy human aging. Arch. Neurol. 1992; 49:1013–1020. [PubMed: 1417508]

Mark CI, Fisher JA, Pike GB. Improved fMRI calibration: precisely controlled hyperoxic versus hypercapnic stimuli. Neuroimage. 2011; 54:1102–1111. [PubMed: 20828623]

McPhee, SJ.; Hammer, GD. Pathophysiology of Disease An Introduction to Clinical Medicine. Sixth Edition. Lange Medical Books; 2009.

Moore R, Berlowitz D, Pretto J, Brazzale D, Denehy L, Jackson B, McDonald C. Acute effects of hyperoxia on resting pattern of ventilation and dyspnoea in COPD. Respirology. 2009; 14:545–550. [PubMed: 19383112]

Ogawa S, Menon RS, Tank DW, Kim S-G, Merkle H, Ellermann JM, Ugurbil K. Functional brain mapping by blood oxygenation level-dependent contrast magnetic resonance imaging. A comparison of signal characteristics with a biophysical model. Biophys. J. 1993; 64:803–812. [PubMed: 8386018]

Ordidge RJ, Gorell JM, Deniau JC, Knight RA, Helpern JA. Assessment of relative brain iron concentrations using T_2-weighted and T_2*-weighted MRI at 3 Tesla. Magn. Reson. Med. 1994; 32:335–341. [PubMed: 7984066]

Perlmutter JS, Powers WJ, Herscovitch P, Fox PT, Raichle ME. Regional asymmetries of cerebral blood flow, blood volume, and oxygen utilization and extraction in normal subjects. J. Cereb. Blood Flow Metab. 1987; 7:64–67. [PubMed: 3492507]

Perthen JE, Lansing AE, Liau J, Liu TT, Buxton RB. Caffeine-induced uncoupling of cerebral blood flow and oxygen metabolism: a calibrated BOLD fMRI study. Neuroimage. 2008; 40:237–247. [PubMed: 18191583]

Roland PE, Eriksson L, Stone-Elander S, Widen L. Does mental activity change the oxidative metabolism of the brain? J. Neurosci. 1987; 7:2373–2389. [PubMed: 3612246]

Severinghaus JW. Simple, accurate equations for human blood O2 dissociation computations. J Appl Physiol. 1979; 46:599–602. [PubMed: 35496]

Sicard KM, Duong TQ. Effects of hypoxia, hyperoxia, and hypercapnia on baseline and stimulus-evoked BOLD, CBF, and CMRO2 in spontaneously breathing animals. Neuroimage. 2005; 25:850–858. [PubMed: 15808985]

Spees WM, Yablonskiy DA, Oswood MC, Ackerman JJ. Water proton MR properties of human blood at 1.5 Tesla: magnetic susceptibility, T_1, T_2, T_2*, and non-Lorentzian signal behavior. Magn. Reson. Med. 2001; 45:533–542. [PubMed: 11283978]

Stankiewicz J, Panter SS, Neema M, Arora A, Batt CE, Bakshi R. Iron in chronic brain disorders: Imaging and neurotherapeutic implications. Neurotherapeutics. 2007; 4:371–386. [PubMed: 17599703]

Uludağ K, Müller-Bierl B, Uğurbil K. An integrative model for neuronal activity-induced signal changes for gradient and spin echo functional imaging. Neuroimage. 2009; 48:150–165. [PubMed: 19481163]

Wismer GL, Buxton RB, Rosen BR, Fisel CR, Oot RF, Brady TJ, Davis KR. Susceptibility induced MR line broadening: applications to brain iron mapping. J Comput Assist Tomogr. 1988; 12:259–265. [PubMed: 3351040]

Xu F, Uh J, Brier MR, Hart J, Yezhuvath US, Gu H, Yang Y, Lu H. The influence of carbon dioxide on brain activity and metabolism in conscious humans. J. Cereb. Blood Flow Metab. 2010; 31:58–67. [PubMed: 20842164]

Yablonskiy DA. Quantitation of intrinsic magnetic susceptibility-related effects in a tissue matrix. Phantom study. Magn. Reson. Med. 1998; 39:417–428. [PubMed: 9498598]

Yablonskiy DA, Haacke EM. Theory of NMR signal behavior in magnetically inhomogeneous tissues: the static dephasing regime. Magn. Reson. Med. 1994; 32:749–763. [PubMed: 7869897]

Zhao JM, Clingman CS, Närväinen MJ, Kauppinen RA, van Zijl PCM. Oxygenation and hematocrit dependence of transverse relaxation rates of blood at 3T. Magn. Reson. Med. 2007; 58:592–597. [PubMed: 17763354]

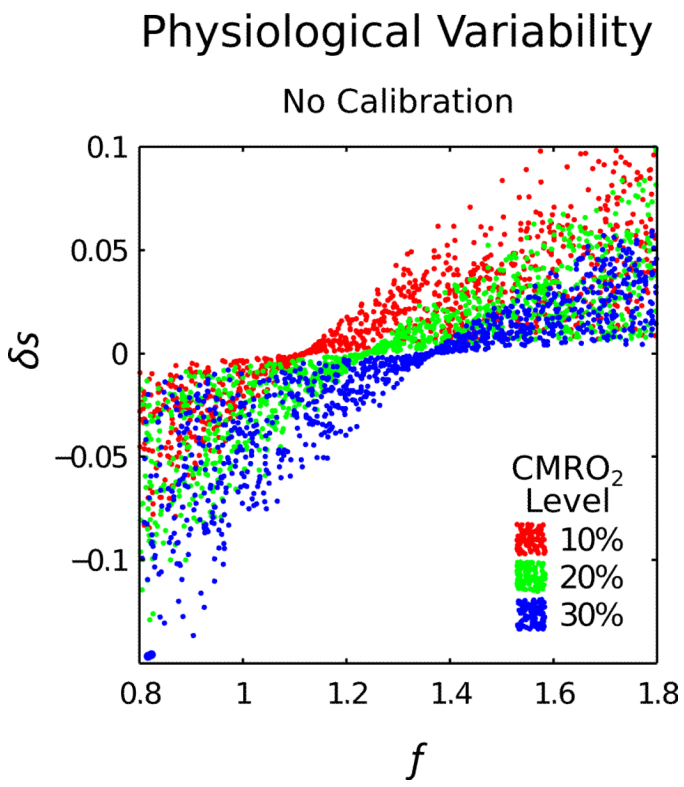

Figure 1.
The effect of physiological variability in haematocrit, baseline oxygen extraction fraction and baseline blood volume on the relationship between the BOLD response (δs) and CBF (f). These simulations show that the effect of physiological variability on δs does not allow 10% step changes in $CMRO_2$ to clearly separated, confirming that this information is insufficient to accurately measure $CMRO_2$.

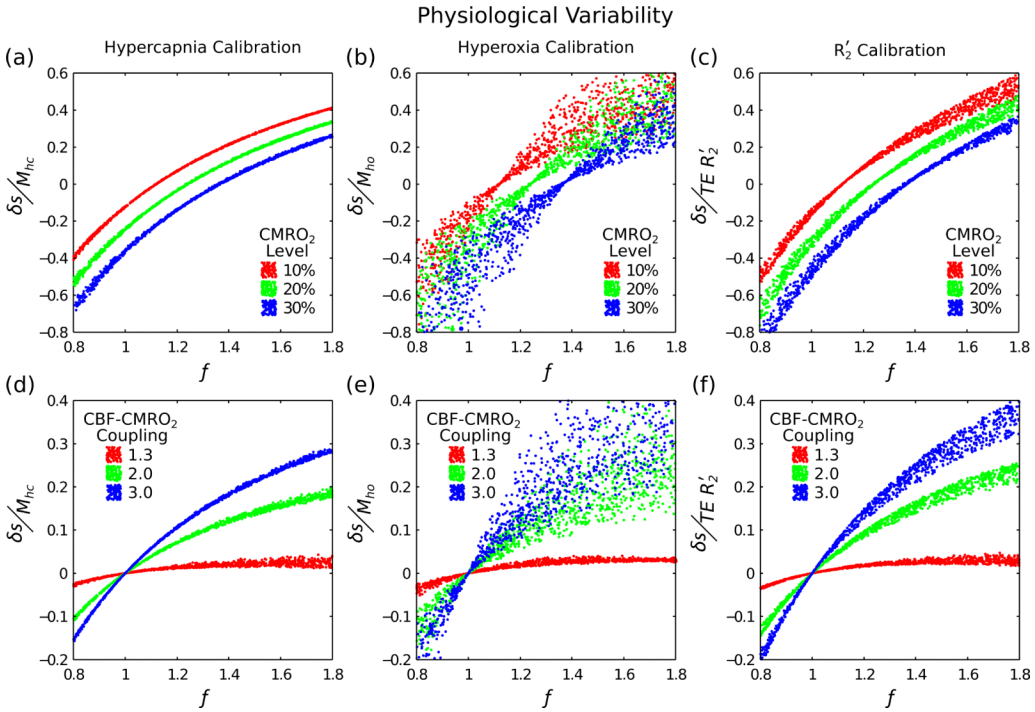

Figure 2.

Three different calibration techniques were investigated to account for physiological variability; hypercapnia, hyperoxia, and R_2' calibration (columns left-right). By simultaneously varying haematocrit (0.37-0.50), oxygen extraction fraction (0.30-0.55) and blood volume (0.01-0.10) we are able to assess how well each method copes with this physiological variability. Simulations were performed for both fixed increases in $CMRO_2$ (top row) and for fixed coupling of CBF and $CMRO_2$ (Eq. (10)) (bottom row). For a perfect calibration each of simulated points should fall on a single curve, which should be distinctly different for each $CMRO_2$ level or CBF-$CMRO_2$ coupling value.

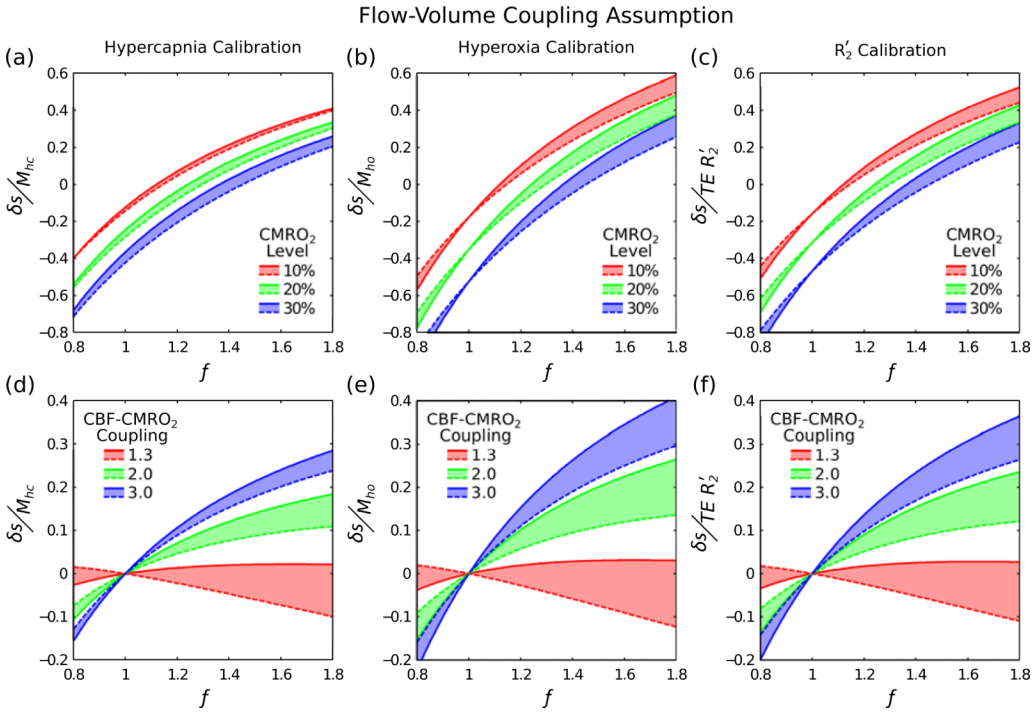

Figure 3.

An inaccurate assumption of the flow-volume coupling constant α would result in a systematic error. Here the effect of different underlying physiological values of this coupling were investigated where a solid line represents α=0.2 and the dashed line α=0.4. A minimal shift in the dashed line with respect to the solid line would reflect lower sensitivity to the assumed value of α. Physiological variability is not included in these simulations and haematocrit, oxygen extraction fraction and blood volume were assumed to be 0.45, 0.4, 0.05, respectively.

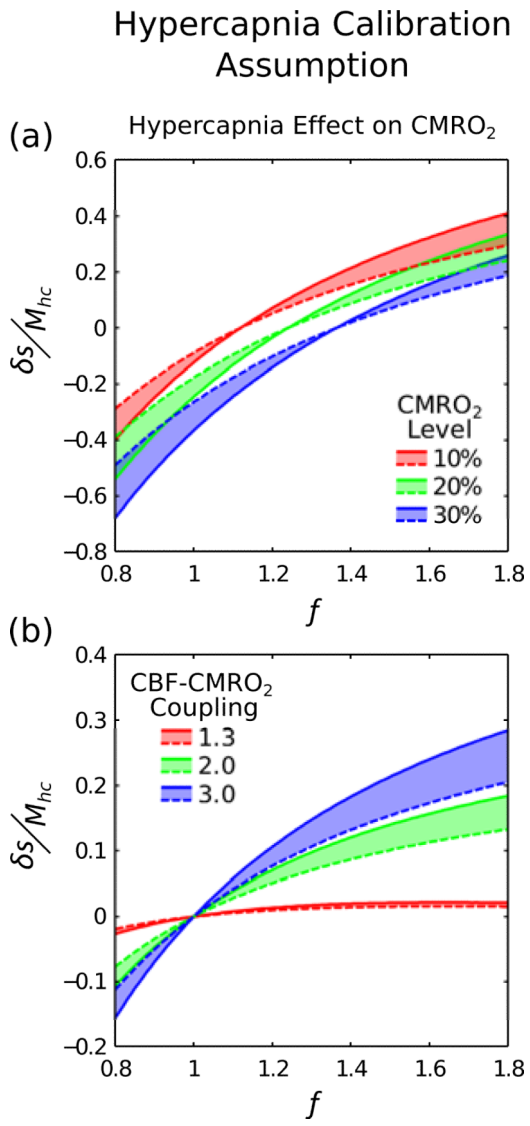

Figure 4.

It has been observed that hypercapnia may cause a reduction in baseline $CMRO_2$. Here we consider what effect this would have on hypercapnia calibration when $CMRO_2$ is reduced by 15% (r=0.85 in Eq. (3)). Physiological variability was not included for clarity. Isometabolism (r=1) is plotted as a solid line whilst reduced $CMRO_2$ is plotted as a dashed line. Shifting of the dashed line with respect to the solid line suggests that reduced baseline $CMRO_2$ would have a marked effect on the accuracy of hypercapnia calibration.

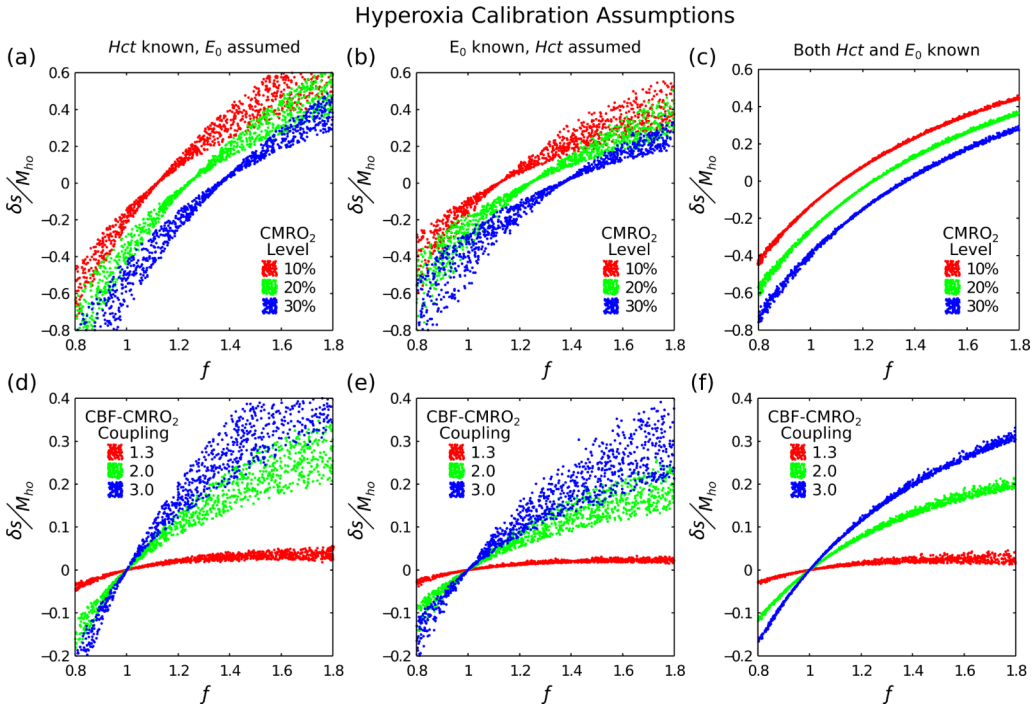

Figure 5.

Further investigation of hyperoxia calibration was undertaken to better understand the large observed variability. This was achieved by increasing the amount of information used to estimate the calibration scaling factor M_{ho}; haematocrit known, oxygen extraction fraction known and both known (columns left-right). Physiological variability was included as it is the origin of the observed variability in Fig. 2b,e. More information about the baseline physiology reduces the variability in hyperoxia calibration.

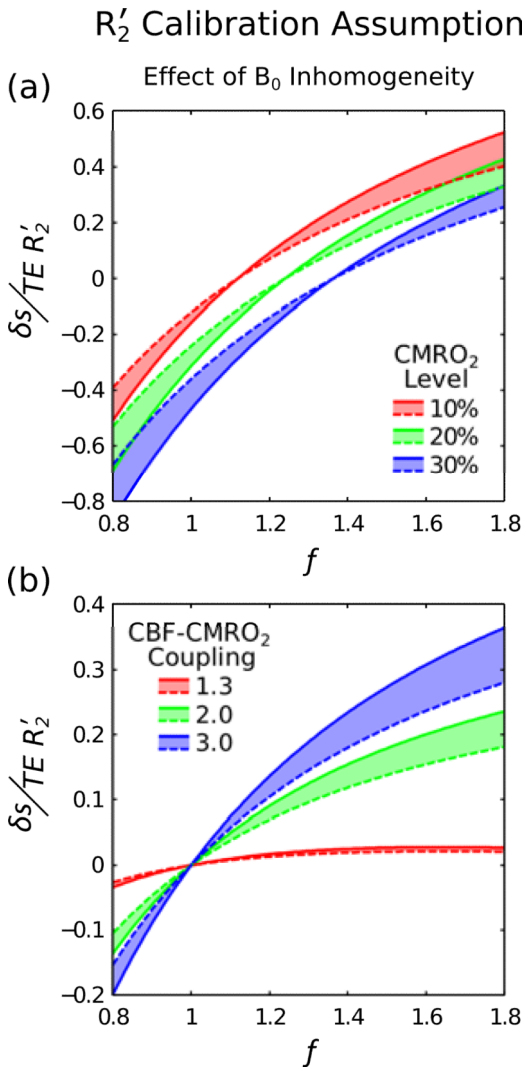

Figure 6.

It is well known that R_2' is sensitive to both mesoscopic and macroscopic sources of magnetic field inhomogeneity. The former represents the effect of blood vessels, which underlies the BOLD response, and the latter is caused by disturbance of the magnetic field by the head. Here we compare perfect field homogeneity ($\Delta\omega=0$), plotted as a solid line, with a through slice gradient $\Delta\omega=20$ Hz, plotted as a dashed line. Shifting of the dashed line with respect to the solid line emphasises that macroscopic field inhomogeneity effects must be minimised.

Table 1

Constants required for the detailed signal model (Griffeth and Buxton, 2011) and extension to simulate R_2'.

Constant	Value	Description
TE	32 ms	Imaging echo time.
ε_A	1.30	Ratio of baseline intravascular arterial to extravascular signal (Griffeth and Buxton, 2011).
ε_C	1.02	Ratio of baseline intravascular capillary to extravascular signal (Griffeth and Buxton, 2011).
ε_V	0.50	Ratio of baseline intravascular venous to extravascular signal (Griffeth and Buxton, 2011).
a_L^*	4.3	Coefficient describing extravascular signal resulting from vessels in the range 16 – 200 μm diameter under a gradient echo (Ogawa et al., 1993).
a_S^*	0.04 s	Coefficient describing extravascular signal resulting from 5 μm diameter vessels under a gradient echo (Ogawa et al., 1993).
$a_{L,5}$	-1.92×10^{-11} s^4	Coefficients describing extravascular signal resulting from 16 μm diameter vessels under a spin echo (Uludağ et al., 2009).
$a_{L,4}$	-1.26×10^{-8} s^3	
$a_{L,3}$	-2.89×10^{-6} s^2	
$a_{L,2}$	2.51×10^{-4} s	
$a_{L,1}$	0.0067	
$a_{L,0}$	-0.0382 s^{-1}	
$a_{S,5}$	-1.13×10^{-11} s^4	Coefficients describing extravascular signal resulting from 5 μm diameter vessels under a spin echo (Uludağ et al., 2009).
$a_{S,4}$	0.96×10^{-8} s^3	
$a_{S,3}$	-3.22×10^{-6} s^2	
$a_{S,2}$	4.90×10^{-4} s	
$a_{S,1}$	-3.58×10^{-6}	
$a_{S,0}$	0.0175 s^{-1}	
Δ	2.64×10^{-7}	Susceptibility of fully deoxygenated blood (Spees et al., 2001).
Y_{off}	0.95	Blood saturation for equal tissue-blood susceptibility (Spees et al., 2001).
$R_{2,0}$	25.1 s^{-1}	Intrinsic transverse relaxation rate for extravascular tissue (Perthen et al., 2008).